A Hydrogen Atom in an Organoplatinum–Amine System. 1. Synthesis and Spectroscopic and Crystallographic Characterization of Novel Zwitterionic Complexes with a Pt(II)$^-$···H–N$^+$ Unit

Ingrid C. M. Wehman-Ooyevaar,[†] David M. Grove,[†] Huub Kooijman,[‡] Paul van der Sluis,[‡] Anthony L. Spek,[‡] and Gerard van Koten*,[†]

Contribution from the Debye Research Institute, Department of Metal-Mediated Synthesis, and Bijvoet Center for Biomolecular Research, Vakgroep voor Kristal- en Structuurchemie, University of Utrecht, Padualaan 8, 3584 CH Utrecht, The Netherlands. *Received May 6, 1992*

Abstract: The unusual bridging-hydrogen complexes PtX(L-*C*,*N*)(LH-*C*,*H*) containing a zwitterionic Pt(II)$^-$···H–N$^+$ moiety have been obtained in a reaction of *cis*-Pt(L-*C*,*N*)$_2$ with R_2SnX_2 (R = Me, Ph; X = Cl, Br) in a mixture of CH_2Cl_2 and MeOH. The chelating amine ligand systems L used in this reaction are $[1\text{-}C_{10}H_6NMe_2\text{-}8]^-$, $[C_6H_4CH_2NMe_2\text{-}2]^-$, and $[C_6H_4CH_2NEt_2\text{-}2]^-$. The complex PtCl(1-$C_{10}H_6NMe_2$-8-*C*,*N*)(1-$C_{10}H_6NHMe_2$-8-*C*,*H*) can also be obtained by reaction of *cis*-Pt(1-$C_{10}H_6NMe_2$-8-*C*,*N*)$_2$ with dry HCl. The bridging proton of the zwitterionic Pt(II)$^-$···H–N$^+$ moiety shows a characteristic ^{1}H NMR resonance at ca. 11–16 ppm with a $^1J(^{195}\text{Pt},^1\text{H})$ of ca. 65–180 Hz; the latter decreases with increasing ligand flexibility. In the Pt···H–N moiety of the PtX(L-*C*,*N*)(LH-*C*,*H*) complexes, an increase of the Pt···H interaction is associated with a simultaneous decrease of the H–N interaction. When L is chiral $[C_6H_4CH(Me)NMe_2\text{-}(R)\text{-}2]^-$, *cis*-Pt(L-*C*,*N*)$_2$ affords in a reaction with Me_2SnBr_2 the nonbridging complex PtBr($C_6H_4CH(Me)NMe_2$-(*R*)-2-*C*,*N*)($C_6H_4CH(Me)NHMe_2$-(*R*)-2-*C*) as the major product. The X-ray crystal structures of both a bridging complex, i.e. PtBr(1-$C_{10}H_6NMe_2$-8-*C*,*N*)(1-$C_{10}H_6NHMe_2$-8-*C*,*H*), and a nonbridging complex, i.e. PtBr($C_6H_4CH(Me)NMe_2$-(*R*)-2-*C*,*N*)($C_6H_4CH(Me)NHMe_2$-(*R*)-2-*C*), are described. Especially the latter shows good evidence that the bridging interaction is largely electrostatic. Internal steric influences only affect the stability of the bridging moiety when they arise from groups on the benzylic carbon atom. Crystal data for PtBr(1-$C_{10}H_6NMe_2$-8-*C*,*N*)(1-$C_{10}H_6NHMe_2$-8-*C*,*H*) at 100 K: $a = 9.469$ (1) Å, $b = 30.481$ (1) Å, $c = 7.298$ (1) Å, $\beta = 91.81$ (1)°, $Z = 4$, $D_{\text{calcd}} = 1.945$ g cm^{-3}, and space group *Cc*. Crystal data for PtBr($C_6H_4CH(Me)NMe_2$-(*R*)-2-*C*,*N*)($C_6H_4CH(Me)NHMe_2$-(*R*)-2-*C*) at 298 K: $a = 11.136$ (1) Å, $b = 12.0577$ (8) Å, $c = 15.378$ (1) Å, $Z = 4$, $D_{\text{calcd}} = 1.841$ g cm^{-3}, and space group $P2_12_12_1$.

Introduction

In the last decade, much research has been done on the activation of C–H bonds by transition metal complexes, and consequently, there is a continuously growing interest in all types of interactions between metal centers and hydrogen atoms.[1] Within the field of C–H activation, the agostic M···H–C interaction has been recognized as a very important one, and many examples of this three-center two-electron interaction are now known.[2,3] Interactions wherein hydrogen is bridging between two metal centers or a metal and nonmetal center, for example M···H–Si,[4] are also of the three-center two-electron type. However, only a few precedents of a M···H–N interaction, being three-center four-electron in character, have been shown in the literature.[5-9] Recently, we presented the isolation and characterization of the first example of an *intra*molecular Pt(II)···H–N interaction in the zwitterionic complexes PtX(1-$C_{10}H_6NMe_2$-8-*C*,*N*)(1-$C_{10}H_6NHMe_2$-8-*C*,*H*) (X = Cl, Br).[5] Other examples of M···H–N interactions had been reported before but are different in being, for example, either *inter*molecular interactions,[6,7] an interaction involving a *neutral* amide function,[8] or an interaction in a cationic moiety.[9] The recognition of the intramolecular M···H–N interaction and its characterization is an important new aspect of organometallic and coordination chemistry. In this study, we detail the characterization of new complexes with a Pt(II)···H–N moiety and report new spectroscopic and structural data which provide further insight into the nature of this interaction. To help identify the factors which are important for the formation and the stability of the Pt···H–N moiety, platinum complexes containing aryl ligands with different rigidity and steric bulk (see Figure 1) have been used as starting materials. Rigidity and steric bulk in the neighborhood of an N-donor atom has been reported to influence the stability and reactivity of platinum,[10] nickel,[11] iridium,[12] and tin complexes.[13]

Experimental Section

General Methods. Syntheses were carried out using standard Schlenk techniques in an atmosphere of purified nitrogen. All solvents were dried and distilled under nitrogen prior to use. The compounds Li($C_6H_4CH(Me)NMe_2$-(*R*)-2-*C*,*N*),[14] $PtCl_2$(cod),[15] $PtCl_2(SEt_2)_2$,[16] *cis*-Pt(1-

---

* To whom correspondence should be addressed.

[†] Debye Research Institute.

[‡] Bijvoet Center for Biomolecular Research.

(1) (a) Janowicz, A. H.; Bergman, R. G. *J. Am. Chem. Soc.* **1983**, *105*, 3929. (b) Jones, W. D.; Feher, F. J. *J. Am. Chem. Soc.* **1984**, *106*, 1650. (c) Crabtree, R. H. *Chem. Rev.* **1985**, *85*, 245. (d) Halpern, J. *Inorg. Chim. Acta* **1985**, *100*, 41. (e) Ryabov, A. D. *Chem. Rev.* **1990**, *90*, 403.

(2) Crabtree, R. H.; Holt, E. M.; Lavin, M.; Morehouse, S. M. *Inorg. Chem.* **1985**, *24*, 1986.

(3) (a) Carr, N.; Dunne, B. J.; Orpen, A. G.; Spencer, J. L. *J. Chem. Soc., Chem. Commun.* **1988**, 926. (b) Brookhart, M.; Green, M. L. H.; Wong, L.-L. *Prog. Inorg. Chem.* **1988**, *36*, 1.

(4) (a) Teller, R. G.; Bau, R. *Struct. Bonding* (*Berlin*) **1981**, *44*, 1. (b) Schubert, U.; Scholz, G.; Müller, J.; Ackermann, K.; Wörle, B.; Stansfield, R. F. D. *J. Organomet. Chem.* **1986**, *306*, 303. (c) Schubert, U. *Adv. Organomet. Chem.* **1990**, *30*, 151.

(5) Wehman-Ooyevaar, I. C. M.; Grove, D. M.; van der Sluis, P.; Spek, A. L.; van Koten, G. *J. Chem. Soc., Chem. Commun.* **1990**, 1367.

(6) Calderazzo, F.; Fachinetti, G.; Marchetti, F.; Zanazzi, P. F. *J. Chem. Soc., Chem. Commun.* **1981**, 181.

(7) Brammer, L.; Charnock, J. M.; Goggin, P. L.; Goodfellow, R. J.; Orpen, A. G.; Koetzle, T. F. *J. Chem. Soc., Dalton Trans.* **1991**, 1789.

(8) Hedden, D.; Roundhill, D. M.; Fultz, W. C.; Rheingold, A. L. *Organometallics* **1986**, *5*, 336.

(9) Cecconi, F.; Ghilardi, C. A.; Innocenti, P.; Mealli, C.; Midollini, S.; Orlandini, A. *Inorg. Chem.* **1984**, *23*, 922.

(10) van Beek, J. A. M.; van Koten, G.; Dekker, G. P. C. M.; Wissing, E.; Zoutberg, M. C.; Stam, C. H. *J. Organomet. Chem.* **1990**, *394*, 659.

(11) van Beek, J. A. M.; van Koten, G.; Ramp, M. J.; Vrieze, K.; Goubitz, K.; Zoutberg, M. C.; Stam, C. H. *Inorg. Chem.* **1991**, *30*, 3059.

(12) (a) Wehman-Ooyevaar, I. C. M.; Grove, D. M.; van Koten, G. To be published. (b) Wehman-Ooyevaar, I. C. M.; Luitwieler, I. F.; Vatter, K.; Grove, D. M.; Smeets, W. J. J.; Horn, E.; Spek, A. L.; van Koten, G. To be published.

(13) (a) van Koten, G.; Jastrzebski, J. T. B. H.; Noltes, J. G.; Pontenagel, W. M. G. F.; Kroon, J.; Spek, A. L. *J. Am. Chem. Soc.* **1978**, *100*, 5021. (b) Oki, M.; Ohira, M. *Chem. Lett.* **1982**, 1267. (c) Jastrzebski, J. T. B. H.; Boersma, J.; van Koten, G. *J. Organomet. Chem.* **1991**, *413*, 43.

(14) van Koten, G.; Jastrzebski, J. T. B. H. *Tetrahedron* **1989**, *45*, 569.

0002-7863/92/1514-9916$03.00/0

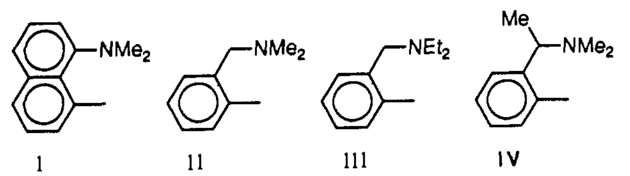

Figure 1. The ligand systems I–IV, varying in rigidity and steric bulk.

$C_{10}H_6NMe_2$-8-*C,N*)$_2$,[17] *cis*- and *trans*-Pt($C_6H_4CH_2NMe_2$-2-*C,N*)$_2$, and *cis*-Pt($C_6H_4CH_2NEt_2$-2-*C,N*)$_2$[18] were prepared by literature methods. ^1H and ^{13}C NMR spectra were recorded on a Bruker AC 200 spectrometer. Infrared spectra were recorded on a Perkin-Elmer 283 infrared spectrophotometer. Elemental analyses were obtained from the Elemental Analyses Section of the Institute for Applied Chemistry TNO, Zeist, The Netherlands, and from Dornis and Kolbe Mikroanalytisches Laboratorium, Mülheim a.d. Ruhr, Germany.

Synthesis of *cis*-Pt($C_6H_4CH(Me)NMe_2$-(*R*)-2-*C,N*)$_2$ (*cis*-1). To a yellow solution of enantiomerically pure Li($C_6H_4CH(Me)NMe_2$-(*R*)-2-*C,N*) (1.09 g; 7 mmol) in Et_2O (40 mL) was added solid $PtCl_2$(cod) (1.32 g; 3.5 mmol). The white suspension was stirred for 18 h and then evaporated in vacuo to dryness. The yellow residue was extracted with CH_2Cl_2 (3 × 30 mL). After concentration of the combined extracts in vacuo to 5 mL, pentane was added (40 mL). The resulting white precipitate was collected by filtration and washed once with pentane (25 mL). The solid was dried in air, affording *cis*-**1** as a white powder (1.5 g; 87% yield). Anal. Calcd for $C_{20}H_{28}N_2Pt$: C, 48.87; H, 5.74; N, 5.70. Found: C, 49.68; H, 5.79; N, 5.64. ^1H NMR ($CDCl_3$, 24 °C): δ 1.72 (d, Ar–CH(C*H*$_3$)–N, $^3J(^1H,^1H) = 6.5$ Hz); 2.71 (s, –NC*H*$_3$, $^3J(^{195}Pt,^1H)$ = 17 Hz); 2.76 (s, –NC*H*$_3$, $^3J(^{195}Pt,^1H) = 12$ Hz); 3.74 (q, Ar–C*H*(CH$_3$)–N, $^3J(^1H,^1H) = 6.5$ Hz); 6.97 (m, 3,4,5-*H* of Ar); 7.52 (d, 6-*H* of Ar, $^3J(^1H,^1H) = 6$ Hz, $^3J(^{195}Pt,^1H) = 65$ Hz). ^{13}C NMR ($CDCl_3$, 24 °C): δ 19.97 (br s, Ar–CH(*C*H$_3$)–N); 46.32 (s, –N*C*H$_3$); 50.90 (s, –N*C*H$_3$); 75.61 (s, Ar–*C*H(CH$_3$)–N, $^2J(^{195}Pt,^{13}C) = 52$ Hz); 120.88 (s, 6-*C* of Ar, $^2J(^{195}Pt,^{13}C) = 40$ Hz); 121.90 (s, 4-*C* of Ar); 125.49 (s, 3-*C* of Ar, $^3J(^{195}Pt,^{13}C) = 88$ Hz); 138.98 (s, 5-*C* of Ar, $^3J(^{195}Pt,^{13}C) = 110$ Hz); 139.82 (s, 1-*C* of Ar, $^1J(^{195}Pt,^{13}C) = 1173$ Hz); 153.51 (s, 2-*C* of Ar, $^2J(^{195}Pt,^{13}C) = 10$ Hz).

Reaction of *trans*-$PtCl_2(SEt_2)_2$ with enantiomerically pure Li($C_6H_4CH(Me)NMe_2$-(*R*)-2-*C,N*) in benzene afforded, after the same workup procedure as described above, a mixture of *cis*-**1** and *trans*-Pt($C_6H_4CH(Me)NMe_2$-(*R*)-2-*C,N*)$_2$ (*trans*-**1**) in a 3:1 ratio that has not been separated into its components. ^1H NMR of *trans*-**1** ($CDCl_3$, 24 °C): δ 1.84 (d, Ar–CH(C*H*$_3$)–N, $^3J(^1H,^1H) = 6.5$ Hz); 3.02 (s, –NC*H*$_3$, $^3J(^{195}Pt,^1H) = 40.8$ Hz); 3.18 (s, –NC*H*$_3$, $^3J(^{195}Pt,^1H) = 43.2$ Hz); 3.64 (br m, Ar–C*H*(CH$_3$)–N); 7.05–7.2 (m, 3,4,5-*H* of Ar); 7.61 (d, 6-*H* of Ar, $^3J(^{195}Pt,^1H)$ not observed).

Synthesis of PtX(L-*C,N*)(LH-*C,H*) (2a: L = 1-$C_{10}H_6NMe_2$-8 (I); X = Cl. 2b: L = 1-$C_{10}H_6NMe_2$-8 (I); X = Br. 3: L = $C_6H_4CH_2NMe_2$-2 (II); X = Br. 4: L = $C_6H_4CH_2NEt_2$-2 (III); X = Br) from R_2SnX_2 (R = Me, Ph; X = Cl, Br) in CH_2Cl_2/MeOH. General Methods. To a solution of *cis*-Pt(L-*C,N*)$_2$ (1–1.5 mmol) in a 10:1 mixture of CH_2Cl_2/MeOH(D) (66 mL) was added a solution of an equimolar amount of R_2SnX_2 in CH_2Cl_2 (10 mL). After being stirred for 1.5 h, this solution was concentrated in vacuo to 3 mL. Upon addition of hexane or ether (40 mL) to the resulting residue, a yellow solid precipitated, and after 0.5 h of stirring, the suspension was filtered off. The solid was washed once with a warm 25:1 mixture of hexane/CH_2Cl_2 (52 mL) and then dried in air, affording the product as an off-white powder. ^1H NMR data, see Table IV.

A. PtCl(1-$C_{10}H_6NMe_2$-8-*C,N*)(1-$C_{10}H_6NHMe_2$-8-*C,H*) (2a): starting from *cis*-Pt(1-$C_{10}H_6NMe_2$-8-*C,N*)$_2$, MeOH, and Me_2SnCl_2, yield 75%.

B. PtCl(1-$C_{10}H_6NMe_2$-8-*C,N*)(1-$C_{10}H_6NHMe_2$-8-*C,H*) (2a): starting from *cis*-Pt(1-$C_{10}H_6NMe_2$-8-*C,N*)$_2$, MeOH, and Ph_2SnCl_2, yield 69%.

C. PtBr(1-$C_{10}H_6NMe_2$-8-*C,N*)(1-$C_{10}H_6NHMe_2$-8-*C,H*) (2b): starting from *cis*-Pt(1-$C_{10}H_6NMe_2$-8-*C,N*)$_2$, MeOH, and Me_2SnBr_2, yield 95%. Anal. Calcd for $C_{24}H_{25}BrN_2Pt$: C, 46.76; H, 4.09; N, 4.54; Br, 12.96. Found: C, 46.32; H, 3.97; N, 4.28; Br, 14.98. Infrared spectra in KBr or NUJOL: ν(N–H) 2100 cm^{-1}. Crystals of **2b**, suitable for a single-crystal X-ray diffraction study, were obtained upon slow evaporation of a CH_2Cl_2/hexane solution of the complex.

D. PtBr(1-$C_{10}H_6NMe_2$-8-*C,N*)(1-$C_{10}H_6NDMe_2$-8-*C,D*) (2b-*d*): starting from *cis*-Pt(1-$C_{10}H_6NMe_2$-8-*C,N*)$_2$, MeOD, and Me_2SnBr_2, yield 67%. Infrared spectrum in KBr: ν(N–D) 1660 cm^{-1}.

E. PtBr($C_6H_4CH_2NMe_2$-2-*C,N*)($C_6H_4CH_2NHMe_2$-2-*C,H*) (3): starting from *cis*-Pt($C_6H_4CH_2NMe_2$-2-*C,N*)$_2$, MeOH, and Me_2SnBr_2, yield 90%. Infrared spectrum in KBr: ν(N–H) 2340 cm^{-1}.

F. PtBr($C_6H_4CH_2NEt_2$-2-*C,N*)($C_6H_4CH_2NHEt_2$-2-*C,H*) (4): starting from *cis*-Pt($C_6H_4CH_2NEt_2$-2-*C,N*)$_2$, MeOH, and Me_2SnBr_2, yield 88%. Infrared spectrum in KBr: ν(N–H) 2300 cm^{-1}.

Reaction of *cis*-Pt(1-$C_{10}H_6NMe_2$-8-*C,N*)$_2$ with Me_2SnBr_2 and 1 Equiv of MeOH. To a solution of *cis*-Pt(1-$C_{10}H_6NMe_2$-8-*C,N*)$_2$ (0.16 g; 0.3 mmol) in CH_2Cl_2 (8 mL) was added MeOH (12.5 μL; 0.3 mmol). Then a solution of Me_2SnBr_2 (0.09 g; 0.3 mmol) in CH_2Cl_2 (3 mL) was added and the resulting solution stirred for 1.5 h. Evaporation in vacuo of the solvent yielded a yellow powder which was, according to its ^1H NMR data, a mixture of *cis*-Pt(1-$C_{10}H_6NMe_2$-8-*C,N*)$_2$, Me_2SnBr_2, **2b**, PtBr(H)(1-$C_{10}H_6NMe_2$-8-*C,N*)$_2$,[19] and PtBr($BrSnMe_2$)(1-$C_{10}H_6NMe_2$-8-*C,N*)$_2$.[19]

Reaction of *cis*-1 (*RR* Diastereoisomer) with Me_2SnBr_2 in CH_2Cl_2/MeOH. Use of the same general procedure as described for the synthesis of **2**–**4** provided a white powder. ^1H NMR data showed this to be a 1:3 mixture of the diastereoisomers PtBr($C_6H_4CH(Me)NMe_2$-(*R*)-2-*C,N*)($C_6H_4CH(Me)NHMe_2$-(*R*)-2-*C,H*) (**5**) and PtBr($C_6H_4CH(Me)NMe_2$-(*R*)-2-*C,N*)($C_6H_4CH(Me)NHMe_2$-(*R*)-2-*C*) (**6**). Recrystallization of this mixture from a 1:10 mixture of CH_2Cl_2 and Et_2O (33 mL) at –20 °C afforded yellow crystals of **6** (0.26 g; 35% yield), suitable for a single-crystal X-ray diffraction study. Anal. Calcd for $C_{20}H_{29}BrN_2Pt$: C, 41.96; H, 5.11; N, 4.89; Br, 13.96. Found: C, 41.38; H, 5.16; N, 4.95; Br, 14.78. Infrared spectrum of **6** in KBr: ν(N–H) 2760 cm^{-1}.

Synthesis of Pt($OOCCF_3$)(1-$C_{10}H_6NMe_2$-8-*C,N*)(1-$C_{10}H_6NHMe_2$-8-*C,H*) (2c). To a yellow solution of **2b** (0.29 g; 0.47 mmol) in a 1:1 mixture of CH_2Cl_2/THF (50 mL) was added dropwise a solution of $AgOOCCF_3$ (0.1 g; 0.46 mmol) in THF (5 mL). Immediately, a white solid formed, and after 10 min of stirring, the mixture was centrifuged; the supernatant solution was then separated by syringe techniques. Upon concentration of this yellow solution to 2 mL, a suspension was formed. The solid was filtered off and washed once with pentane (10 mL). Drying in air afforded **2c** as an off-white powder (0.2 g; (67% yield).

Reaction of Me_2SnBr_2 with MeOH. A. To a solution of Me_2SnBr_2 (0.03 g; 0.1 mmol) in $CDCl_3$ (0.5 mL) was added an excess of MeOH. The ^1H NMR spectrum was subsequently recorded and followed in time. No reaction was observed.

B. To a solution of Me_2SnBr_2 (0.03 g; 0.1 mmol) in $CDCl_3$ (0.5 mL) was added a 4-fold excess of $C_6H_5CH(Me)NMe_2$-(*R*). Then an excess of MeOH was added, and immediately, a white solid precipitated. Upon addition of DMSO-d_6 (0.3 mL), a clear solution was obtained. The ^1H NMR spectrum was subsequently recorded and followed in time. A broad signal at 4.3 ppm and broad signals around 0.7 ppm appeared and increased in time.

Reaction of *cis*-Pt(1-$C_{10}H_6NMe_2$-8-*C,N*)$_2$ and HCl. A. Through a yellow, slightly turbid, solution of *cis*-Pt(1-$C_{10}H_6NMe_2$-8-*C,N*)$_2$ (0.58 g; 1.1 mmol) in CH_2Cl_2 (15 mL) was bubbled dry gaseous HCl for 5 min. The resulting clear dark-yellow solution was evaporated in vacuo to a brownish sticky residue. Pentane (15 mL) was added and the suspension stirred for 18 h. Filtration of this suspension yielded a light-yellow powder, which was washed once with pentane (10 mL). Drying in air afforded 0.66 g of a light-yellow powder, which was identified as the salt [$C_{10}H_7NHMe_2$-8][$PtCl_2$(1-$C_{10}H_6NMe_2$-8-*C,N*)] by its ^1H NMR data. ^1H NMR ($CDCl_3$, 24 °C): δ 3.62 (s, –NC*H*$_3$, 12 H, $^3J(^{195}Pt,^1H) = 43$ Hz, intensity 6%); 7.2–7.4 (m, –*H* of Ar, 3 H); 7.4–7.8 (m, –*H* of Ar, 7 H); 7.94 (d, –*H* of Ar, 1 H, $J(^1H,^1H) = 5.6$ Hz); 7.99 (d, –*H* of Ar, 1 H, $J(^1H,^1H) = 7.5$ Hz); 8.88 (d, –*H* of Ar, 1 H, $J(^1H,^1H) = 7.5$ Hz); 12.1 (br s, –N*H*, 1 H). Traces of PtCl(H)(1-$C_{10}H_6NMe_2$-8-*C,N*)$_2$ were also present in the spectrum.[19]

Upon storage of this solid for several hours in air and at room temperature, another product was formed: ^1H NMR ($CDCl_3$, 24 °C): δ 3.52 (s, –NC*H*$_3$, 12 H, $^3J(^{195}Pt,^1H) = 43$ Hz, intensity 6%); 7.1–7.6 (m, –*H* of Ar, 9 H); 7.73 (d, –*H* of Ar, 1 H, $J(^1H,^1H) = 7$ Hz); 7.85 (d, –*H* of Ar, 1 H, $J(^1H,^1H) = 8.5$ Hz); 8.78 (d, –*H* of Ar, 1 H, $J(^1H,^1H) = 8.5$ Hz); 11.6 (br s, –N*H*, 1 H). A trace of PtCl(H)(1-$C_{10}H_6NMe_2$-8-*C,N*)$_2$ was also present in this spectrum.[19]

B. In a typical NMR experiment, a yellow solution of ca. 25 mg of *cis*-Pt(1-$C_{10}H_6NMe_2$-8-*C,N*)$_2$ in 1 mL of dry $CDCl_3$ was prepared. Through this solution was bubbled for ca. 2 s an excess of dry HCl. The ^1H NMR spectrum of the resulting yellow solution showed formation of a 3:1 mixture of **2a** (see Table IVa) and the salt [$C_{10}H_7NHMe_2$-8][$PtCl_2$(1-$C_{10}H_6NMe_2$-8-*C,N*)], i.e. the product of method A described

---

(15) Clark, H. C.; Manzer, L. E. *J. Organomet. Chem.* **1973**, *59*, 411.

(16) Kaufmann, G. B.; Corvan, D. O. *Inorg. Synthesis* **1960**, *6*, 211.

(17) Wehman, E.; van Koten, G.; Knaap, I. C.; Ossor, H.; Pfeffer, M.; Spek, A. L. *Inorg. Chem.* **1988**, *27*, 4409.

(18) Longoni, G.; Fantucci, P.; Chini, P.; Canzioni, F. *J. Organomet. Chem.* **1972**, *39*, 413.

(19) Part 2: Wehman-Ooyevaar, I. C. M.; Grove, D. M.; de Vaal, P.; Dedieu, A.; van Koten, G. *Inorg. Chem.*, in press.

above. No traces of $PtCl(H)(1\text{-}C_{10}H_6NMe_2\text{-}8\text{-}C,N)_2$ were observed.[19]

Reaction of $C_{10}H_7NMe_2$-8 with HCl. Through a solution of $C_{10}H_7NMe_2$-8 in pentane was bubbled dry gaseous HCl for 5 min. Immediately, a white solid precipitated. The suspension was evaporated to dryness in vacuo to afford a white powder, which was identified by its ^1H NMR data as the salt $[C_{10}H_7NHMe_2\text{-}8][Cl]$. ^1H NMR ($CDCl_3$, 24 °C): δ 3.4 (s, $-N(CH_3)_2$, 6 H); 7.4–7.65 (m, $-H$ of Ar, 2 H); 7.65–7.85 (m, $-H$ of Ar, 2 H); 7.9 (d, $-H$ of Ar, 1 H, $J(^1H,^1H) = 8.5$ Hz); 7.92 (d, $-H$ of Ar, 1 H, $J(^1H,^1H) = 8.5$ Hz); 8.92 (d, $-H$ of Ar, 1 H, $J(^1H,^1H) = 8.5$ Hz); 13.8 (br s, $-NH$, 1 H).

Reactions of 2 with Basic or Electrophilic Reagents. A. Proton Sponge. To a yellow solution of **2b** (0.11 g; 0.18 mmol) in CH_2Cl_2 (20 mL) was added a solution of Proton Sponge (0.04 g; 0.18 mmol) in CH_2Cl_2 (5 mL). After the yellow solution was stirred for 3.5 h, a sample was taken and its ^1H NMR spectrum showed that protonation of Proton Sponge had occurred for 15%. The solution was stirred for another 3 days and then evaporated to dryness in vacuo to afford a yellow powder. The ^1H NMR spectrum showed that protonation of Proton Sponge had taken place for 43%.

B. D_2O. To a solution of **2b** (5 mg) in $CDCl_3$ (0.5 mL) was added D_2O (0.05 mL), and after being vigorously shaken for 3 min, the resulting mixture was measured by ^1H NMR; this showed that no reaction had occurred.

C. NaOH. A solution of NaOH (0.1 g; 2.5 mmol) in EtOH (15 mL) was added to a yellow solution of **2c** (0.23 g; 0.35 mmol) in CH_2Cl_2 (25 mL). After 1 h of stirring, the resulting brownish solution was evaporated to dryness in vacuo. This residue was extracted with CH_2Cl_2 (30 mL) and the yellow extract evaporated in vacuo to afford a yellow residue. This solid was washed once with pentane (10 mL) and dried in air to afford *cis*-$Pt(1\text{-}C_{10}H_6NMe_2\text{-}8\text{-}C,N)_2$ as a yellow powder (0.16 g; 85% yield).

D. Pyridine-d_5. To a solution of **2c** (5 mg) in $CDCl_3$ (0.5 mL) was added pyridine-d_5 (0.05 mL) and the resulting solution measured by ^1H NMR; this showed the quantative formation of *cis*-$Pt(1\text{-}C_{10}H_6NMe_2\text{-}8\text{-}C,N)_2$.

E. MeI. To a yellow solution of **2a** (**2b**) (0.24 g; 0.4 mmol) in CH_2Cl_2 (10 mL) was added freshly distilled MeI (25 μL; 0.4 mmol). After 2 h of stirring, the yellow solution was evaporated in vacuo to afford a yellow powder. This was dried in air and was identified by its ^1H NMR data as **2a** (**2b**). Prolongation of the reaction time (1–4 days) did not change the result.

X-Ray Data Collection, Structure Determination, and Refinement of $PtBr(1\text{-}C_{10}H_6NMe_2\text{-}8\text{-}C,N)(1\text{-}C_{10}H_6NHMe_2\text{-}8\text{-}C,H)$ (2b). A rod-shaped yellow crystal was mounted on a glass fiber and transferred to an Enraf-Nonius CAD4F diffractometer for data collection at 100 K. Unit cell parameters were determined from a least squares fit of the SET4 setting angles of 25 reflections with $12.4 < \theta < 19.3°$ and were checked for the presence of higher lattice symmetry.[20] Data were corrected for Lp and for absorption (ABSORB,[21] correction range 2.45–3.11); no decay occurred during the 81 h of X-ray exposure time. Standard deviations as obtained by counting statistics were increased according to an analysis of the excess variance of the free reference reflections: $\sigma^2(I) = \sigma_{cs}^2(I) + (0.013I)^2$.[22] The structure was solved by automated Patterson methods followed by peak optimization (SHELXS86).[23] Refinement on F was carried out by full matrix least squares techniques (SHELX76).[24] Hydrogen atoms were introduced at calculated positions (C–H = 0.98 Å), except for H(1), which was located from a difference Fourier and refined (U = 0.01 (1) Å^2). All non-hydrogen atoms were refined with anisotropic thermal parameters. All other hydrogen atoms were refined with one isotropic thermal parameter (U = 0.025 (7) Å^2). Weights were introduced in the final refinement cycles; convergence was reached at R = 0.016. Refinement of the alternative absolute structure converged at R = 0.027 and R_w = 0.034.

Crystal data and numerical details of the structure determination are given in Table I. Neutral atom scattering factors were taken from ref 25 and corrected for anomalous dispersion.[26] All calculations were performed on a MicroVAX cluster. The EUCLID package was used for geometrical calculations and illustrations.[27] Full listings of atomic parameters, thermal parameters for all atoms, and bond lengths and angles and listings of observed and calculated structure factor amplitudes for **2b** are supplied as supplementary material (Tables S1–S5).

Table I. Crystal Data and Details of the Structure Determination for **2b** and **6**

	2b	**6**
	a. Crystal Data	
formula	$C_{24}H_{25}BrN_2Pt$	$C_{20}H_{29}BrN_2Pt$
mol wt	616.46	572.45
cryst syst	monoclinic	orthorhombic
space group	*Cc* (No. 9)	$P2_12_12_1$ (No. 19)
a, Å	9.469 (1)	11.136 (1)
b, Å	30.481 (1)	12.0577 (8)
c, Å	7.298 (1)	15.378 (1)
β, deg	91.81 (1)	
V, Å^3	2105.3 (4)	2065.0 (3)
Z	4	4
D_{calc}, g cm^{-3}	1.945	1.841
$F(000)$, electrons	1184	1104
μ(Mo Kα), cm^{-1}	86.2	87.9
cryst dimen, mm	0.13 × 0.13 × 0.26	0.5 × 0.5 × 0.3
	b. Data Collection and Refinement	
temp, K	100	298
radiation, Å	Mo Kα (Zr-filter), 0.71073	Mo Kα (Zr-filter), 0.71073
θ_{max}, deg	29.4	27.5
scan type	$\omega/2\theta$	$\omega/2\theta$
$\Delta\omega$, deg	$0.65 + 0.35 \tan\theta$	$0.83 + 0.35 \tan\theta$
Hor and vert aperture, mm	3.0, 5.0	2.88, 4.00
dist cryst to detector, mm	173	173
ref reflections	$22\bar{1}$, $1\bar{3}0$, $0\bar{2}\bar{1}$	224, $22\bar{4}$, $\bar{3}02$
data set	h 0:13; k −38:40; l −10:10	−14:14; 0:15; 0:19
total data	5353	3494
total unique data	2917	3323
obs data	2781 ($I > 2.5\sigma(I)$)	2248 ($I > 2.5\sigma(I)$)
No. of refined parameters	256	237
weighting scheme	$w = 1.0/\sigma^2(F)$	$w = 1.0/\sigma^2(F)$
final R, R_w, S	0.016, 0.016, 1.83	0.042, 0.038, 2.75
$(\Delta/\sigma)_{max}$ in final cycle	0.29	0.337
min and max resd dens, e Å^{-3}	−0.71, 0.84	−1.49, 1.28

X-Ray Data Collection, Structure Determination, and Refinement of $PtBr(C_6H_4CH(Me)NMe_2\text{-}(R)\text{-}2\text{-}C,N)(C_6H_4CH(Me)NHMe_2\text{-}(R)\text{-}2\text{-}C)$ (6). Crystal data and numerical details of the structure determination are given in Table I. A yellow, block-shaped crystal, suitable for X-ray structure determination, was mounted on a Lindemann glass capillary and transferred to an Enraf-Nonius CAD4F diffractometer for data collection. Lattice parameters were determined by least squares fitting of the SET4 setting angles of 25 reflections with $10.8 < \theta < 19.1°$. The unit cell parameters were checked for the presence of higher lattice symmetry.[20] All data were collected with $\omega/2\theta$ scan mode. Data were corrected for Lp and for the observed linear decay (<2%) of the reference reflections during 53 h of X-ray exposure time. Absorption correction was applied using Gaussian integration techniques (ABSORB,[21] correction range 8.20 to 18.49). Standard deviations of the intensities as obtained by counting statistics were increased according to an analysis of the excess variance of the reference reflections: $\sigma^2(I) = \sigma_{cs}^2(I) + (0.034I)^2$.[22] The structure was solved by automated Patterson methods (SHELXS86).[23] Refinement on F was carried out by full matrix least squares techniques (SHELX76).[24] The hydrogen atoms were included in the refinement on calculated positions (C–H = 0.98 Å) riding on their carrier atoms, except for H(24), which was located from a difference Fourier map and subsequently refined. All non-hydrogen atoms were refined with anisotropic thermal parameters; the hydrogen atoms were refined with two common isotropic thermal parameters, one for the methyl groups, except C(4), and one for the other hydrogen atoms, of 0.12 (2) and 0.062 (11) Å^2, respectively. Weights were introduced in the final refinement cycles. Convergence was reached at R = 0.042 and R_w = 0.038. The absolute configuration was checked by refinement of the alternative chirality, which resulted in an R value of 0.050; R_w = 0.048. Neutral atom scattering factors were taken from ref 25; anomalous-

---

[20] Spek, A. L. *J. Appl. Crystallogr.* **1988**, *21*, 578.

[21] Spek, A. L. ABSORB, Program for Absorption Correction; University of Utrecht, The Netherlands, ECM Abstracts Book, 1983; p 283.

[22] McCandlish, L. E.; Stout, G. H.; Andrews, L. C. *Acta Crystallogr.* **1975**, *A31*, 245.

[23] Sheldrick, G. M. SHELXS86. Program for Crystal Structure Determination. University of Göttingen, Federal Republic of Germany, 1986.

[24] Sheldrick, G. M. SHELX76. Program for Crystal Structure Determination. Cambridge University, England, 1976.

[25] Cromer, D. T.; Mann, J. B. *Acta Crystallogr.* **1968**, *A24*, 321.

[26] Cromer, D. T.; Liberman, D. *J. Chem. Phys.* **1970**, *53*, 1891.

[27] Spek, A. L. *Acta Crystallogr.* **1990**, *A46*, C34.

dispersion corrections from ref 26. Geometric calculations and illustrations were performed with PLATON.[27] Calculations were carried out on a DEC system 5000. Full listings of atomic parameters, thermal parameters for all atoms, and bond lengths and angles and listings of observed and calculated structure factor amplitudes for **6** are supplied as supplementary material (Tables S1–S5).

Results

Synthesis and Characterization of *cis*- and *trans*-Pt(C_6H_4CH(Me)NMe$_2$-(*R*)-2-*C*,*N*)$_2$ (1). The synthesis of *cis*-Pt(C_6H_4CH(Me)NMe$_2$-(*R*)-2-*C*,*N*)$_2$ (*cis*-**1**) in high yield was carried out in a transmetalation reaction by treating PtCl$_2$(cod) with 2 equiv of Li(C_6H_4CH(Me)NMe$_2$-(*R*)-2-*C*,*N*), see eq 1. Complex *cis*-**1** is air-stable and soluble in most common organic solvents; it is not soluble in pentane and is slightly soluble in diethyl ether. The complex has been characterized by ^{1}H and ^{13}C NMR (see Experimental Section), and the combined data are consistent with a square-planar Pt(II) structure, in which both chelating ligands are cis positioned.[17,18] As a consequence of the enantiomerically pure C,N ligand, the Me groups of the two –CH(Me)– moieties are on opposite sides of the coordination plane.

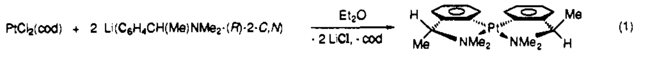

cis-**1**

Since complex *cis*-**1** was made from the enatiomerically pure [C_6H_4CH(Me)NMe$_2$-(*R*)-2]$^-$ ligand, this platinum complex is formed as a single *RR* diastereoisomer. In its ^{1}H NMR spectrum (CDCl$_3$, 24 °C, 200 MHz), the most characteristic data are the two singlets for the Me protons of the –NMe$_2$ group with different $^3J(^{195}\text{Pt},^1\text{H})$ values of 12 and 17 Hz and a low-field doublet at 7.52 ppm (with $^3J(^{195}\text{Pt},^1\text{H})$ of 65 Hz) that is assigned to the proton positioned ortho to the metal center. The platinum–proton spin–spin coupling constant values in *cis*–**1** are similar to those of achiral *cis*-Pt($C_6H_4CH_2$NMe$_2$-2-*C*,*N*)$_2$.[18]

When *trans*-PtCl$_2$(SEt$_2$)$_2$ instead of PtCl$_2$(cod) is reacted with Li(C_6H_4CH(Me)NMe$_2$-(*R*)-2-*C*,*N*), a mixture of *cis*–**1** and its trans isomer (*trans*-**1**) is formed. The most important difference between the ^{1}H NMR spectra of *cis*–**1** and *trans*-**1** is the value of the ^{195}Pt coupling constants on the –NMe$_2$ singlets, with the values of 41 and 43 Hz for *trans*-**1** being comparable to those found for *trans*-Pt($C_6H_4CH_2$NMe$_2$-2-*C*,*N*)$_2$.[18] In the proposed square-planar structure for *trans*-**1** (*RR* diastereoisomer), both Me groups of the –CH(Me)– moieties point to the same side of the coordination plane. These synthetic results indicate that *cis*-**1** is thermodynamically more stable than *trans*-**1**; this observation has parallels in the related synthesis of, for example, *cis*- and *trans*-Pt($C_6H_4CH_2$NMe$_2$-2-*C*,*N*)$_2$[18] or *cis*-Pt($CH_2C_6H_4$NMe$_2$-2-*C*,*N*)$_2$.[28]

Synthesis and Characterization of the Bridging-Hydrogen Complexes PtX(L-*C*,*N*)(LH-*C*,*H*) (2–6). Upon treatment of the Pt(II) complexes *cis*-Pt(L-*C*,*N*)$_2$ (L = I, II, or III) with R$_2$SnX$_2$ (R = Me, Ph; X = Cl, Br) in a 10:1 mixture of CH$_2$Cl$_2$ and MeOH, the unique bridging-hydrogen complexes PtX(L-*C*,*N*)(LH-*C*,*H*) (**2a**, L = I, X = Cl; **2b**, L = I, X = Br; **3**, L = II, X = Br; **4**, L = III, X = Br) were formed in yields between 70 and 95%, see reaction 2 in Scheme I. When MeOD was used instead of MeOH in the reaction with Me$_2$SnBr$_2$ (L = I), the deuterium analogue of **2b**, i.e. PtBr(1-$C_{10}H_6$NMe$_2$-8-*C*,*N*)(1-$C_{10}H_6$NDMe$_2$-8-*C*,*D*) (**2b**–*d*), was obtained.

From the reaction of *cis*-Pt(1-$C_{10}H_6$NMe$_2$-8-*C*,*N*)$_2$ and Me$_2$SnBr$_2$ carried out with a stoichiometric amount of MeOH (1 equiv per equiv of Pt complex instead of a 10-fold excess) in the same time as in reaction 2, a mixture containing not only the starting materials but also **2b**, PtBr(H)(1-$C_{10}H_6$NMe$_2$-8-*C*,*N*)$_2$, and PtBr(Me$_2$SnBr)(1-$C_{10}H_6$NMe$_2$-8-*C*,*N*)$_2$ was obtained.[19] Another method to obtain **2a** is the addition of gaseous HCl to *cis*-Pt(1-$C_{10}H_6$NMe$_2$-8-*C*,*N*)$_2$; see reaction 4 in Scheme I. The CF$_3$COO analogue of **2a**, i.e. Pt(OOCCF$_3$)(1-$C_{10}H_6$NMe$_2$-8-*C*,*N*)(1-$C_{10}H_6$NHMe$_2$-8-*C*,*H*) (**2c**), was formed in 67% yield starting from **2a**(**b**) in an anion-exchange reaction with AgOOCCF$_3$; see reaction 3 in Scheme I.

Scheme I. Synthetic Routes for PtX(L-*C*,*N*)(LH-*C*,*H*)

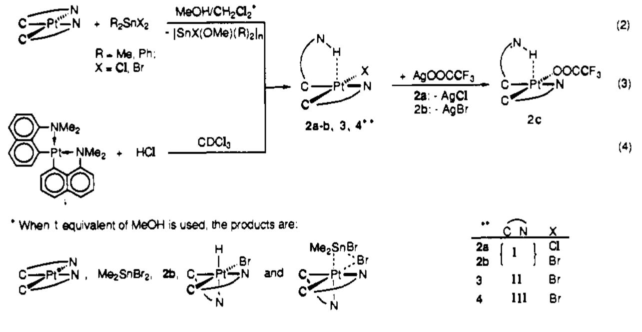

Reaction 2 with *cis*-Pt(C_6H_4CH(Me)NMe$_2$-(*R*)-2-*C*,*N*)$_2$ (*cis*-**1**) provides a mixture of two diastereoisomers, i.e. the bridging-hydrogen complex PtBr(C_6H_4CH(Me)NMe$_2$-(*R*)-2-*C*,*N*)(C_6H_4CH(Me)NHMe$_2$-(*R*)-2-*C*,*H*) (**5**) and the nonbridging isomer PtBr(C_6H_4CH(Me)NMe$_2$-(*R*)-2-*C*,*N*)(C_6H_4CH(Me)NHMe$_2$-(*R*)-2-*C*) (**6**), in a ratio varying from 1:3 to 1:15; see eq 5.

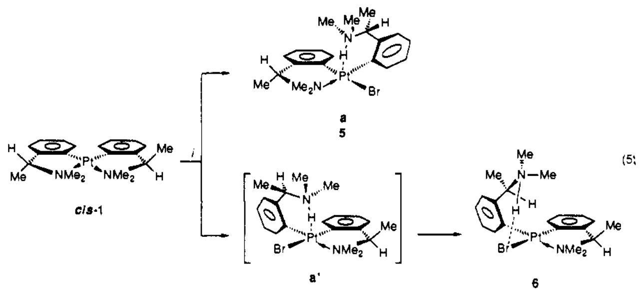

i) + Me$_2$SnBr$_2$; MeOH/CH$_2$Cl$_2$; - [SnBr(OMe)(Me)$_2$]$_n$; product ratio of **5** and **6** varies between 1:3 and 1:15.

Finally, when the trans isomer of Pt($C_6H_4CH_2$NMe$_2$-2-*C*,*N*)$_2$ was treated with Me$_2$SnBr$_2$ in a CH$_2$Cl$_2$/MeOH mixture, no bridging-hydrogen complex was formed. A reaction took place, but the Pt product has not yet been identified.

Complexes **2a**, **2b**, and **2c** have low solubilities in common organic solvents, whereas **3** and **4** dissolve reasonably well in CH$_2$Cl$_2$ and CHCl$_3$ but only slightly in benzene. Complex **6** dissolves in all common organic solvents, except for Et$_2$O, pentane, and hexane. All complexes **2**, **3**, **4** and **6** are air-stable in the solid state, but in solution they slowly decompose to unidentified materials. The complexes **2**, **3**, **4**, and **6** have been identified primarily by ^{1}H NMR and IR spectroscopy; both **2b** and **6** have been further characterized by elemental analysis and an X-ray structure determination.

The reactions (2) also provide a tin complex that crystallizes out of hexane at low temperature. The ^{1}H NMR spectrum of this product shows a broad singlet at 3.3 ppm and two broad multiplets at ~0.8 and ~1.3 ppm (with Sn satellites for R = Me). On the basis of these data and the stoichiometry of the reaction, this tin complex is proposed to be [SnX(OMe)(R)$_2$] (X = Cl, Br; R = Me, Ph), which could be either monomeric or dimeric depending on the concentration of the solution.[29]

^{1}H NMR and IR Spectroscopy of 2. The ^{1}H NMR spectra of **2a**, **2b**(-*d*), and **2c** are very similar; see Table II. The two –NMe$_2$ groups provide four separate Me signals, of which two are doublets ($^3J(^1\text{H},^1\text{H})$ = 6 Hz) without ^{195}Pt satellites (for **2b**-*d* two singlets; $^3J(^2\text{D},^1\text{H})$ not resolved) and the other two are broad singlets with platinum satellites that appear as shoulders. Furthermore, in the aromatic region there are two doublet resonances; one at high field (6.27 ppm) and one at low field (8.39 ppm) assigned to the aromatic ortho protons. These data point to an asymmetric structure for **2** in which the naphthyl ligands are perpendicular to each other.[30] However, the most distinctive aspect of the ^{1}H

---

(28) van der Ploeg, A. F. M. J.; van Koten, G.; Vrieze, K.; Spek, A. L. *Inorg. Chem.* **1982**, *21*, 2014.

(29) Chapman, A. C.; Davies, A. G.; Harrison, P. G.; McFarlane, W. *J. Chem. Soc. C* **1970**, 821.

Table II. ^1H NMR Data of the Zwitterionic Hydrogen Complexes $PtX(1\text{-}C_{10}H_6NMe_2\text{-}8\text{-}C,N)(1\text{-}C_{10}H_6NHMe_2\text{-}8\text{-}C,H)$ (**2**)[a]

X (complex)	aryl-H H(2) H(2)′	aryl-H others	$NHMe_2$[b]	NMe_2[c]	Pt···H[d]
Cl (**2a**)	6.34 d (78) 8.41 d (72)	6.88 t (16) 7.23–7.72 m 7.92 d	2.66 d (6) 3.32 d (6)	3.52 s 3.56 s	15.88 (180)
Br (**2b**)	6.27 d (78) 8.39 d (72)	6.89 t (15) 7.28–7.69 m 7.92 d	2.64 d (6) 3.33 d (6)	3.59 s	15.78 (176)
Br (**2b**-*d*)	6.27 d (78) 8.39 d (72)	6.89 t (15) 7.28–7.7 m 7.92 d	2.64 s 3.34 s	3.56 s 3.58 s	
$OOCCF_3$ (**2c**)	6.19 d (75) 8.39 d (69)	6.81 t (15) 7.26–7.72 m 7.94 d	2.48 d (6) 3.39 d (6)	3.41 s 3.42 s	15.77 (150)

[a] Recorded in $CDCl_3$ at RT; δ in ppm relative to external TMS; $^nJ(^{195}Pt,^1H)$ in Hz in parentheses unless otherwise stated. [b] $^3J(^1H,^1H)$ in parentheses; no $^4J(^{195}Pt,^1H)$ present. [c] $^3J(^{195}Pt,^1H)$ not resolved. [d] Broad singlet.

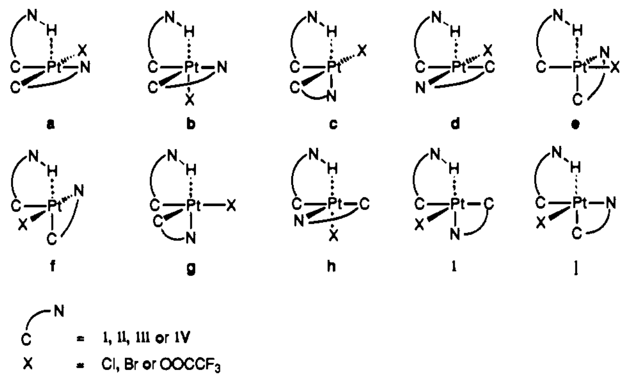

Figure 2. The 10 possible stereoisomeric forms of PtX(Y)(L-*C,N*)(LH-*C,H*). Complexes **2**–**4** have most likely geometry a; see text.

NMR spectra is a broad singlet resonance at low field (15.8 ppm) with a ^{195}Pt coupling constant of ca. 180 Hz (for **2c** 150 Hz). For **2b**-*d* this resonance is not present in its ^1H NMR spectrum. This low-field resonance and its coupling to platinum together with the doublet Me resonances of one $-NMe_2$ unit all point to a hydrogen atom with protonic character, that not only is bonded to a N atom but is also interacting with the metal center. We are dealing here with an unusual interaction of a d^8 metal with an $-HNMe_2$ group that forms a Pt···H–N bridging unit. The interactions within this unit are very strong, and when **2b** is treated with D_2O, there is no evidence for H/D exchange. The IR spectra of complexes **2b** and **2b**-*d* (see Experimental Section) are those to be anticipated for a Pt···H–N structural unit. There is a broad absorption band at 2100 cm^{-1} for the N–H bond in **2b** which is at lower frequency than the N–H absorption of free tertiary ammonium salts (ca. 2700 cm^{-1}).[31] For **2b**-*d*, the broad N–D absorption is, as expected, at a lower frequency, i.e. 1660 cm^{-1}.

In the ^1H NMR spectra of complexes **2**, the aromatic ortho protons exhibit ^{195}Pt coupling constant values of 75 Hz that point to a formal platinum oxidation state of 2+. In Pt(IV) complexes with two naphthyl ligands, the corresponding values are in the range 30–40 Hz.[30] The oxidation state of 2+ has been confirmed for **2b** by X-ray photoelectron spectroscopy measurements.[32] In general, for a Pt(II) complex, a four-coordinate square-planar geometry is normal. However, for **2** ($PtX(1\text{-}C_{10}H_6NMe_2\text{-}8\text{-}C,N)(1\text{-}C_{10}H_6NHMe_2\text{-}8\text{-}C,H)$ (X = Cl, Br, or $OOCCF_3$)), a description in terms of a square-planar geometry is not applicable, because we deal here with two nonidentical, mutually perpendicular naphthyl ligands that are C,N and C,H bonded to platinum. Taking the anionic group X as the fifth ligand and an empty coordination place as the sixth, the Pt(II) complexes **2a**, **2b**(-*d*), and **2c** can be described as octahedral complexes PtX(Y)(L-*C,N*)(LH-*C,H*) (X = Cl, Br, or $OOCCF_3$; Y = empty place), which can exist in 20 stereoisomeric forms, consisting of 10 pairs of enantiomers a–h; see Figure 2.[33]

However, on the basis of primarily spectroscopic data, it is possible to eliminate structures c–j as being those of the isolated products. For example, structures i and j do not have perpendicular naphthyl systems, and the nonresolved Pt coupling con-

Table III. Selected Data on the Geometry of $PtBr(1\text{-}C_{10}H_6NMe_2\text{-}8\text{-}C,N)(1\text{-}C_{10}H_6NHMe_2\text{-}8\text{-}C,H)$ (**2b**) and $PtBr(C_6H_4CH(Me)NMe_2\text{-}(R)\text{-}2\text{-}C,N)(C_6H_4CH(Me)NHMe_2\text{-}(R)\text{-}2\text{-}C)$ (**6**)

Bond Distances (Å)

2b		**6**	
Pt–C(1)	1.995 (5)	Pt–C(10)	1.969 (12)
Pt–N(1)	2.193 (4)	Pt–N(1)	2.165 (10)
Pt–C(13)	1.993 (5)	Pt–C(20)	1.998 (13)
Pt–Br	2.5316 (6)	Pt–Br	2.5236 (17)
Pt···N(2)	2.982 (4)	Pt···N(2)	3.283 (12)
Pt···H(1)	2.11 (5)	Pt···H(24)	2.446 (12)
N(2)–H(1)	0.88 (5)	N(2)–H(24)	0.980 (17)
		Br···H(24)	2.486 (13)
		Br···N(2)	3.411 (13)
		Pt···C(13)	3.264 (14)
		Pt···H(131)	2.987 (15)

Bond Angles (deg)

2b		**6**	
C(1)–Pt–N(1)	82.77 (16)	C(10)–Pt–N(1)	82.0 (5)
C(1)–Pt–C(13)	93.56 (19)	C(10)–Pt–C(20)	92.3 (5)
C(1)–Pt–Br	174.74 (14)	C(10)–Pt–Br	173.9 (4)
C(1)–Pt···H(1)	92.0 (1.2)	C(10)–Pt···H(24)	126.3 (5)
N(1)–Pt–C(13)	176.21 (16)	N(1)–Pt–C(20)	174.3 (5)
N(1)–Pt–Br	93.05 (9)	N(1)–Pt–Br	94.2 (3)
N(1)–Pt···H(1)	107.3 (1.2)	N(1)–Pt···H(24)	113.9 (4)
C(13)–Pt–Br	90.56 (13)	C(20)–Pt–Br	91.5 (4)
C(13)–Pt···H(1)	73.7 (1.2)	C(20)–Pt···H(24)	68.8 (5)
Br–Pt···H(1)	92.3 (1.2)	Br–Pt···H(24)	59.7 (3)
Pt···H(1)–N(2)	168 (4)	Pt···H(24)–N(2)	140.4 (1.4)
		C(10)–Pt···H(131)	76.7 (5)
		N(1)–Pt···H(131)	117.0 (4)
		C(20)–Pt···H(131)	60.4 (5)
		Br–Pt···H(131)	109.4 (3)
		Br···H(24)–N(2)	157.4 (1.5)

---

(30) van Beek, J. A. M.; van Koten, G.; Wehman-Ooyevaar, I. C. M.; Smeets, W. J. J.; van der Sluis, P.; Spek, A. L. *J. Chem. Soc., Dalton Trans.* **1991**, 883.

(31) Hesse, M.; Meier, H.; Zeeh, B. *Spektroskopische Methoden in der Organischen Chemie*; Georg Thieme Verlag: Stuttgart–New York, 1987; Table 2.5.

(32) Monochromatic X-ray photoelectron spectroscopy (XPS) was used for determination of the Pt 4f binding energy of the Pt center in **2b**. Apparatus and methods are described in a publication dealing with XPS data of the Pt complexes $[PtX(C_6H_3(CH_2NMe_2)_2\text{-}2,6)]$: Muijsers, J. C.; Niemantsverdriet, J. W.; Wehman-Ooyevaar, I. C. M.; Grove, D. M.; van Koten, G. *Inorg. Chem.* **1992**, *31*, 2655.

(33) Purcell, F. K.; Kotz, J. C. *Inorganic Chemistry*; W. B. Sanders Company: Philadelphia–London–Toronto, 1977; p 619.

Table IV. ^{1}H NMR Data of the Zwitterionic Hydrogen Complexes $PtBr(C_6H_4CH(R)NR'_2\text{-}2\text{-}C,N)(C_6H_4CH(R)NHR'_2\text{-}2\text{-}C,H)$ (**3**–**6**)[a]

R/R′ (complex)	aryl-H[b] H(6) H(6)′	CH(R)NHR′$_2$[c,d]	CH(R)NR′$_2$[d]	NHR′$_2$[c]	NR′$_2$[e]	Pt···H[f]
H/Me (**3**)	6.35 d (78)	3.98 dd (6.5)	3.76 d (16)	2.66 d (5.4)	2.94 s	11.54 (75)
	7.82 d (69)	4.12 dd (4.2)	4.09 d (21)	2.72 d (5.4)	2.96 s	
H/Et (**4**)	6.43 d (74)	3.89 dd (5.8)	3.67 d (16)	1.04 t (7)	1.28 t (7)[c]	11.35 (66)
	7.95 d (68)	4.02 dd (7.4)	3.93 d[e]	1.53 t (7)	1.33 t (7)[c]	
				2.8–3.3 m	3.3–3.5 m	
Me/Me (**5**)[g]	6.36 d (78)	5.28 q (6.9)	3.82 q (6.2)[c]	2.20 d (5.6)		12.75 (104)
	7.88 d (64)			2.79 d (5.6)		
Me/Me (**6**)	6.30 d (81)	1.51 d (6.9)	1.54 d (6.2)[c]	2.41 d (5.6)	2.84 s (17)	10.90
	7.97 d (66)	5.01 q (6.9)	3.86 q (6.2)[c]	2.89 d (5.6)	2.99 s (14)	

[a] Recorded in $CDCl_3$ at RT; δ in ppm relative to external TMS; $^nJ(^{195}Pt,^1H)$ in Hz in parentheses unless otherwise stated. [b] Others are multiplet resonances from 6.7–7.2 ppm. [c] $^3J(^1H,^1H)$ in parentheses; no $^4J(^{195}Pt,^1H)$ present. [d] For R = H; AB pattern with $^2J(^1H,^1H)$ = 11.6–14.2 Hz. [e] $^3J(^{195}Pt,^1H)$ not resolved when not given. [f] Broad singlet. [g] NMR data obtained from a spectrum of the mixture of **5** and **6** by selection based on relative peak intensities. The resonances which are not given are obscured by those of **6**.

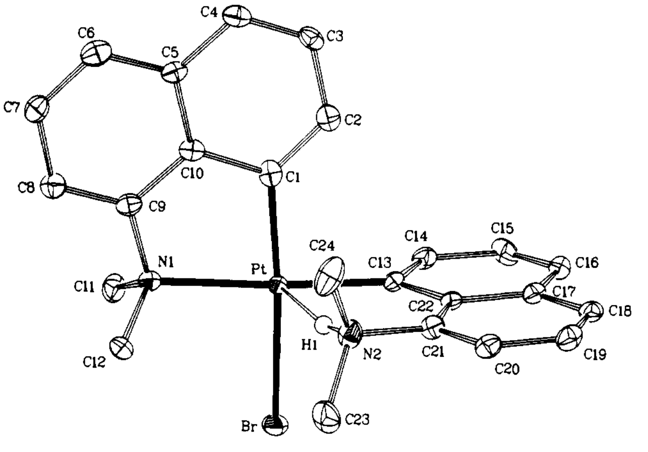

Figure 3. ORTEP plot of the molecule $PtBr(1\text{-}C_{10}H_6NMe_2\text{-}8\text{-}C,N)(1\text{-}C_{10}H_6NHMe_2\text{-}8\text{-}C,H)$ (**2b**) with adopted labeling drawn at the 50% probability level.

stants on the NMe singlets are in the range for those found for –NMe groups trans to C-ligands (40–50 Hz).[18,30] Because an unambiguous stereoisomeric discrimination between a and b did not seem possible with the available NMR data, we have determined an X-ray structure of one of these complexes. The solid-state structure of complex **2b** has geometry a, and we assume that complexes **2a** and **2c** also have this (a) geometry.

Solid-State Structure of $PtBr(1\text{-}C_{10}H_6NMe_2\text{-}8\text{-}C,N)(1\text{-}C_{10}H_6NHMe_2\text{-}8\text{-}C,H)$ (2b). The X-ray structure of **2b** together with the adopted numbering scheme is shown in Figure 3. The bond lengths and angles are listed in Table III. In a square plane around the platinum center are coordinated a C,N-chelating $1\text{-}C_{10}H_6NMe_2\text{-}8$ ligand (via C(1) and N(1)), a bromide atom (Br) cis to N(1), and a protonated $1\text{-}C_{10}H_6NHMe_2\text{-}8$ ligand monodentate C-bonded (via C(13)) cis to C(1); ∠C(1)–PtC(13) = 93.56 (19)°. This last ligand is orientated almost perpendicular to the square plane with the $-NHMe_2$ unit occupying a fifth coordination site above the platinum center, which lies only 0.041 (9) Å out of the square plane toward this unit. For the C,N-chelating system, the distances Pt–C(1) (1.995 (5) Å) and Pt–N(1) (2.193 (4) Å) and the angle C(1)–Pt–N(1) (82.77 (16)°) are comparable to those in the starting material *cis*-$Pt(1\text{-}C_{10}H_6NMe_2\text{-}8\text{-}C,N)_2$.[34] These bond lengths are in accordance with the Pt center being in the oxidation state 2+; in the Pt(IV) complex *trans,cis*-$PtI_2(1\text{-}C_{10}H_6NMe_2\text{-}8\text{-}C,N)_2$, in which the two *N,N*-dimethylnaphthylamine ligands are cis to each other, the corresponding Pt–C and Pt–N distances are significantly longer than those in **2b**.[18] For the C(13)-bonded naphthylamine system (Pt–C(13) = 1.993 (5) Å) there is no Pt–N bond (Pt···N(2) = 2.982 (4) Å). A proton bonded to this noncoordinating N(2) center (N(2)–H(1) = 0.88 (5) Å) makes it a quaternary ammonium salt, and there is a Pt···H(1) distance of 2.11 (5) Å. This is rather long compared to the normal range of 1.51–1.8 Å for a covalent Pt–H bond,[35] but it is shorter than the Pt···H distance of 2.318 (22) Å in *cis*-$Pt(o\text{-}Ph_2PC_6H_4NC(O)C_6H_4)(o\text{-}Ph_2PC_6H_4NHC(O)Ph)$, which was assigned as an intramolecular Pt···H–N interaction.[8] Thus, we conclude that in **2b** an intramolecular interaction between platinum and hydrogen is present. This interaction is part of an almost linear three-center arrangement (∠Pt···H(1)–N(2) = 168 (4)°). We might, in fact, consider this second naphthylamine ligand to be chelating via C(13) and H(1) wherein this bridging H atom occupies a pseudooctahedral position.

^{1}H NMR and IR Spectroscopy of 3–6. The ^{1}H NMR spectra of **3**–**5** show the same characteristics as those of **2** (vide supra) concerning the aromatic region and the N substituents; see Table IV. However, the spectra are more complicated due to the resonances of the benzylic moiety. In the spectra of **3** and **4**, the two benzylic resonances of the ligand that is C,NH coordinated both appear as doublets of doublets (without Pt satellites) as a result of mutual geminal coupling and further coupling to the amine NH proton at 11.5 ppm (confirmed by homonuclear decoupling).

The most striking aspect of the spectra of **3**, **4**, and **5** is the characteristic position of the bridging amine proton. Whereas the resonance in **2** was at ca. 16 ppm, now in **3**, **4**, and **5**, this is at 11.5, 11.4, and 12.75 ppm, respectively. Such a shift to higher field implies a smaller interaction with the metal center. Even more indicative for a decreased interaction are the smaller $^1J(^{195}Pt,^1H)$ values of 75, 66, and 104 Hz, respectively (180 Hz in **2**). Furthermore, in the IR spectra (see Experimental Section), the absorption band of the N–H bond in **3** and **4** is shifted to higher frequency (ca. 2300 vs 2100 for **2b**), and this implies a greater N–H bonding character attended by a decreased interaction with the Pt center. This result was confirmed by ^{15}N-filtered ^{1}H NMR measurements of the complexes **2b** and **3**: the latter has a $^{15}N-^1H$ coupling constant of 69 Hz, which is significantly larger than that of **2b** ($^1J(^{15}N,^1H)$ = 59 Hz).[36] Nevertheless, from the ^{195}Pt coupling constants, it is clear that an interaction is still present, and on the basis of the combined spectroscopic data, the structures of **3** and **4** are proposed to have the same stereoisomeric form as given for **2**, i.e. geometry a. As mentioned above, this structure exists as a pair of enantiomers, which give only one pattern in NMR spectroscopy. However, complex **5** contains two additional chiral centers, i.e. the benzylic C atoms, and geometry a is one of two possible diastereoisomers, the other being a′ in eq 5. The ^{1}H NMR spectrum of **5** shows only one pattern, and therefore this complex exists as only one

---

(34) van Beek, J. A. M.; Grove, D. M.; Smeets, W. J. J.; Spek, A. L.; van Koten, G. To be published.

(35) (a) Auburn, M.; Ciriano, M.; Howard, J. A. K.; Murray, M.; Pugh, N. J.; Spencer, J. L.; Stone, F. G. A.; Woodward, P. *J. Chem. Soc., Dalton Trans.* **1980**, 659. (b) Chiang, M. Y.; Bau, R.; Minghetti, G.; Bandini, A. L.; Banditelli, G.; Koetzle, T. F. *Inorg. Chem.* **1984**, *23*, 122. (c) Hackett, M.; Ibers, J. A.; Jernakoff, P.; Whitesides, G. M. *J. Am. Chem. Soc.* **1986**, *108*, 8094. (d) Michelin, R. A.; Bertani, R.; Mozzon, M.; Zanotto, L.; Benetollo, F.; Bombieri, G. *Organometallics* **1990**, *9*, 1449.

(36) Rüegger, H.; Pregosin, P. S.; Wombacher, F.; van Koten, G.; Grove, D. M.; Wehman-Ooyevaar, I. C. M. *Magn. Reson. Chem.* **1992**, *30*, 548.

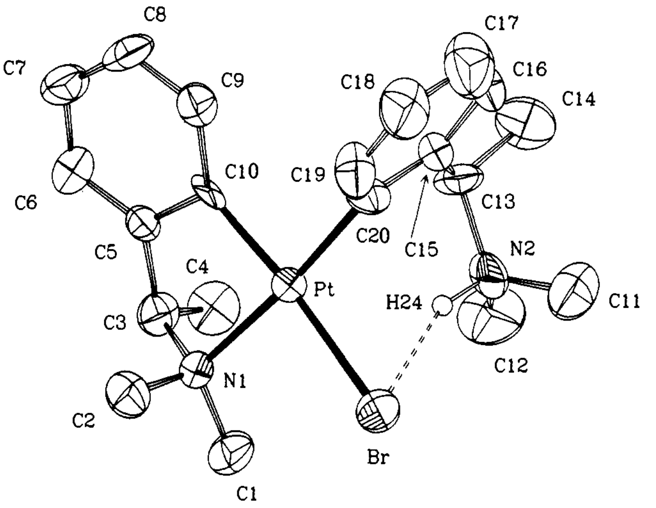

Figure 4. ORTEP plot of the molecule $\mathrm{PtBr(C_6H_4CH(Me)NMe_2}$-(*R*)-2-*C*,*N*)$\mathrm{(C_6H_4CH(Me)NHMe_2}$-(*R*)-2-*C*) (6) with adopted labeling drawn at the 50% probability level.

of these stereoisomeric structures. We believe **5** to have structure a because in structure a′ there would be significant steric hindrance present between the ammonium moiety and the Me substituent of the bidentate ligand.

In the ^{1}H NMR spectrum of **6**, the amine proton shows a resonance at 10.9 ppm without ^{195}Pt satellites. All the other resonance positions and Pt coupling constants in the spectrum are very similar to those of **3**, **4**, and **5**. Compared to **2**, **3**, and **4**, complex **6** has an IR spectrum (see Experimental Section) in which a ν(N–H) (at 2760 cm^{-1}) is shifted to much higher frequency. Based on these data and the fact that the free protonated ligand $\mathrm{[C_6H_4CH(Me)NHMe_2}$-(*R*)-2]$\mathrm{[OOCCF_3]}$ has a ^{1}H NMR resonance at 11.55 ppm for the amine proton, a structure for **6** is proposed with the opposite diastereoisomeric form to that established for **5**; this structure has a "free" ammonium moiety and not a bridging amine hydrogen interaction; see eq 5. Experimental support for the proposed "free" ammonium moiety is obtained in the reaction of **6** with $\mathrm{D_2O}$. Whereas no H/D exchange was found for **2**, for **6** it begins immediately and was complete within 3 h. Because the $\mathrm{HNMe_2}$ unit is moved away from the platinum center, the benzylic proton (with a resonance at 5.01 ppm) could be involved in a Pt···H–C interaction.[37] To investigate this aspect and how the charges are divided in this zwitterionic complex, the molecular geometry of **6** has been determined by an X-ray diffraction analysis.

Solid-State Structure of $\mathbf{PtBr(C_6H_4CH(Me)NMe_2}$-(*R*)-2-*C*,*N*)$\mathbf{(C_6H_4CH(Me)NHMe_2}$-(*R*)-2-*C*) (6). Figure 4 shows the X-ray structure of **6** together with the adopted numbering scheme. The bond lengths and angles are listed in Table III. As in **2b**, the complex has a square-planar geometry in which the platinum center is surrounded by a C,N-chelating $\mathrm{C_6H_4CH(Me)NMe_2}$-(*R*)-2 ligand (via aryl C(10) and N(1)), Br (cis to N(1)), and the $\mathrm{C_{aryl}}$-atom C(20) of a monodentate-bonded protonated ligand $\mathrm{C_6H_4CH(Me)NHMe_2}$-(*R*)-2. The distances (Å) from these ligating atoms to the Pt center are all in their usual range. The aryl ligands are cis positioned and perpendicular to each other as in the structure of **2b**, and the monodentate C-bonded ligand also contains a related quaternary ammonium moiety ($\mathrm{HNMe_2R}$) with N(2)–H(24) = 0.980 (17) Å. However, in **6** the distance between N(2) and Pt is very long (3.283 (12) Å) and the NH proton (H(24)) and the Pt center are separated by 2.469 (12) Å. Compared to the case of **2b**, the ammonium moiety in **6** has turned out of the Pt coordination sphere and the ammonium proton H(24) is now only 2.486 (13) Å from the Br atom. We might say that the protonic H points to the middle of the Pt–Br bond, so indicating the presence of negative charge in that area. The distance between Pt and the benzylic H (Pt···H(131) = 2.987 (15) Å) is too long to represent a significant bonding interaction. In contrast to the case of **2b**, no real pseudooctahedral position is occupied and the angles which H(24) or H(131) make with the meridional plane all deviate significantly from 90° (see Table III).

Scheme II. Reactivity of **2** toward Basic Reagents

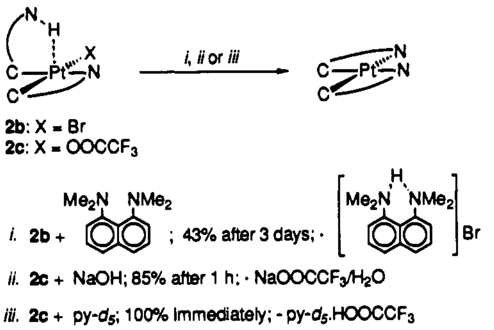

Reactions of *cis*-$\mathbf{Pt(1\text{-}C_{10}H_6NMe_2}$-8-*C*,*N*)$_2$ with HCl. Upon treating a $\mathrm{CDCl_3}$ solution of *cis*-$\mathrm{Pt(1\text{-}C_{10}H_6NMe_2}$-8-*C*,*N*)$_2$ with gaseous HCl, the bridging-hydrogen complex **2a** is formed as the major product (see reaction 4 in Scheme I), together with small amounts of another complex. This latter complex is formed quantitatively when a large excess of HCl is used. On the basis of its NMR data and that of the salt $\mathrm{[C_{10}H_7NHMe_2}$-8][Cl] (see Experimental Section), this complex is probably the salt $\mathrm{[C_{10}H_7NHMe_2}$-8]$\mathrm{[PtCl_2(1\text{-}C_{10}H_6NMe_2}$-8-*C*,*N*)].

Reactions of 2 with Basic or Electrophilic Reagents. Reactions with basic reagents, summarized in Scheme II, and the chemical shift of the H atom in the Pt···H–N unit show the acidic character of the bridging hydrogen atom in complexes **2**. The extremely strong, but bulky, base Proton Sponge (1,8-bis(dimethylamino)naphthalene) deprotonates **2b** in $\mathrm{CDCl_3}$ only slowly over a period of several days. Thus, the bridging H atom appears to be tightly bonded, and this is consistent with the presence of $^{1}J(^{195}\mathrm{Pt},^{1}\mathrm{H})$ on this atom. However, with smaller bases like hydroxide or pyridine, deprotonation occurs immediately.

Surprisingly, **2a** (**2b**) with its zwitterionic character does not react with the strong electrophile MeI at room temperature. For **2b**, the zwitterionic character implies an increased nucleophilicity of the Pt center compared to that of the starting material *cis*-$\mathrm{Pt(1\text{-}C_{10}H_6NMe_2}$-8-*C*,*N*)$_2$, which reacts with a variety of electrophilic reagents, e.g. $\mathrm{I_2}$ or MeI.[17,30] The fact that the reaction of **2b** with MeI did not take place might be attributed to the ortho proton of the protonated ligand, which blocks the only free reactivity site of the Pt center.

Discussion

Formation of the Bridging-Hydrogen Complexes 2–4. Mechanism of the $\mathbf{R_2SnX_2}$/MeOH Reaction. A number of experiments have been carried out to help elucidate the formation of the unusual bridging-hydrogen complexes **2**–**4** from the reaction of *cis*-Pt(L-*C*,*N*)$_2$ with $\mathrm{R_2SnX_2}$ in the presence of MeOH, which is overall an addition of HX to *cis*-Pt(L-*C*,*N*)$_2$. The use of MeOD in reaction 2 (to form the deuterium analogue **2b**-*d*) shows that the protonic H originates from the methanol. Formation of **2b**-*d* indirectly via **2b** in an H/D-exchange reaction with MeOD is unlikely, since **2b** shows no H/D exchange with $\mathrm{D_2O}$. For the formation of **2**–**4**, two possible first steps can be envisaged: (i) generation of HX from $\mathrm{R_2SnX_2}$ and MeOH or (ii) an (oxidative) addition of $\mathrm{R_2SnX_2}$ to the d^{8} metal center to give an intermediate like $\mathrm{PtX(R_2SnX)}$(L-*C*,*N*)$_2$.[19,38,39] In our system, step ii is probably

---

(37) (a) Miller, R. G.; Stauffer, R. D.; Fahey, D. R.; Parnell, D. R. *J. Am. Chem. Soc.* **1970**, *92*, 1511. (b) van der Poel, H.; van Koten, G.; Vrieze, K. *Inorg. Chem.* **1980**, *19*, 1145. (c) Anklin, C. G.; Pregosin, P. S. *Magn. Reson. Chem.* **1985**, *23*, 671.

(38) van der Zeijden, A. A. H.; van Koten, G.; Wouters, J. M. A.; Wijsmuller, W. F. A.; Grove, D. M.; Smeets, W. J. J.; Spek, A. L. *J. Am. Chem. Soc.* **1988**, *110*, 5354.

(39) (a) Kuiper, J. *Inorg. Chem.* **1977**, *16*, 2171; **1978**, *17*, 77. (b) Butler, G.; Eaborn, C.; Pidcock, A. *J. Organomet. Chem.* **1979**, *181*, 47. (c) Packett, D. L.; Syed, A.; Trogler, W. C. *Organometallics* **1988**, *7*, 159. (d) Holt, M. S.; Wilson, W. L.; Nelson, J. H. *Chem. Rev.* **1989**, *89*, 11. (e) Schubert, U.; Kunz, E.; Harkers, B.; Willnecker, J.; Meyer, J. *J. Am. Chem. Soc.* **1989**, *111*, 2572.

not operative; ^{1}H NMR studies gave no evidence for such tin-containing intermediates, and the reaction of *cis*-Pt(1-$C_{10}H_6NMe_2$-8-*C,N*)$_2$ and Me_2SnX_2 *with* MeOH to form **2** is much faster than the reaction *without* MeOH that leads to other products.[19] Therefore, we conclude that the first step in the formation of **2–4**, *for the MeOH reaction*, is the reaction of R_2SnX_2 with MeOH to generate HX and $R_2SnX(OMe)$;[40,41] see eq 6. This conclusion is fully consistent with the fact that *cis*-Pt(1-$C_{10}H_6NMe_2$-8-*C,N*)$_2$ reacts with HCl to give the bridging-hydrogen complex (**2a**).

R_2SnX_2 (R = Me, Ph; X = Cl, Br) + MeOH $\rightleftharpoons$

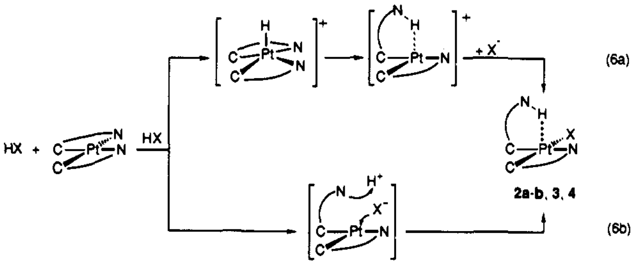

The R_2SnX_2/MeOH system is an excellent HX donor only when a base is present (see Experimental Section), and to obtain HX exclusively as the first step, it is also essential that an excess of ROH is present; with only 1 equiv of MeOH, reaction 2 gives a mixture of **2b** and its tautomer the Pt(IV) hydride PtBr(H)(1-$C_{10}H_6NMe_2$-8-*C,N*)$_2$ (see ref 19).

In reaction 2, it is the Pt(II) complexes, which possess two basic centers (Pt and N), that are believed to be acting as bases to promote the formation of HX. Reactions of HX with d^8 organometallic complexes are widely known and can proceed not only by an oxidative addition reaction at the metal center,[42] but also by electrophilic attack at the metal–carbon bond[43] and by reaction at the coordinated ligand.[44] The end products of reaction 2, i.e. **2–4**, show only N-protonation of the ligand, but this is probably not a result of direct attack of HX at the ligand. We believe that the first step in the reaction of *cis*-Pt(L-*C,N*)$_2$ with HX is either the nucleophilic attack of the filled Pt(II) $d_z{}^2$ orbital on the H$^{\delta+}$ atom of HX in an S_N2 type of mechanism to form a five-coordinate square-pyramidal Pt(IV) intermediate [PtH(L-*C,N*)$_2$]$^+$ (see eq 6a) or the electrophilic attack of X$^-$ at the Pt center to result in N-dissociation and formation of [PtX(L-*C,N*)$_2$]$^-$ (see eq 6b). We do not have kinetic data to discriminate between these two pathways, but (6b) has our preference because it affords in one step the orientation found in the final zwitterionic products and does not include an energetically unfavorable sequence of oxidative addition and reductive elimination reactions as in (6a). In route 6b, attack of X$^-$ on *cis*-Pt(L-*C,N*)$_2$ forces the N atom to dissociate and the ligand can then rotate about the Pt–C_{ipso} bond, to allow protonation of the noncoordinated N atom and formation of the zwitterionic product. The lithium chloride induced acidolysis of $PdCl(C_6H_4CH_2NEt_2$-2-*C,N*)(PPh_3), containing a Lewis basic Pd center, has also been proposed to follow such a route to generate the zwitterionic intermediate $PdCl_2(C_6H_4CH_2NHEt_2$-2-*C*)(PPh_3).[45] Both in this case and in our system, where the platinum center also has Lewis base character, one would not normally expect electrophilic attack; X$^-$ addition followed by protonation is usually found for Lewis acid metal centers as in [IrL$_n$(cod)][PF$_6$][42b] and IrCl(L)(cod).[46]

For the formation of **5** and **6**, a mechanism analogous to that shown in eq 6b, i.e. HBr formation from Me_2SnBr_2 and MeOH followed by its addition to **1**, is also likely to be operative.

Steric Influences on the Formation and Stability of the Hydrogen Bridge. Since the three ligands, I, II, and III provide the bridging-hydrogen complexes PtX(L-*C,N*)(LH-*C,H*) (**2–4**), there is a minimal influence of internal steric hindrance present on the N-donor atom, either on the course of the syntheses or on the stability of the products. In the proposed mechanism of eq 6b, it makes no difference which of the bidentate ligands I, II, or III turns 90° during attack of X$^-$ to form the anionic complex [PtX(L-*C,N*)$_2$]$^-$; i.e. both enantiomers represented by structure a may be formed in the second (protonation) step. During the formation of **5** from *cis*-Pt($C_6H_4CH(Me)NMe_2$-(*R*)-2-*C,N*)$_2$, in which the bidentate ligand L (IV) is chiral, rotation of one of the ligands (the first step) gives another diastereoisomer than rotation of the other; the two diastereoisomers which result are represented by a and a′ in eq 5. Only one diastereoisomer *with* a bridging Pt(II)···H–N unit, i.e. **5**, is obtained, and we conclude that it has structure a (with the same Pt geometry as found for **2b**) and not structure a′, wherein the bridging moiety would be destabilized by the steric influence of the Me substituent of the *bi*dentate C,N ligand. What we find, therefore, is that monodentate ligand in a′ turns its –HNMe$_2$ moiety out of the Pt coordination sphere and creates, as identified in the solid-state structure of **6**, a new type of N–H 'bridging' interaction in which the proton is above the Pt–Br bond. This structure points to an important electrostatic component to the bridging interaction not only in this complex but also in **2–5**.

The differences in the strength of the bridging Pt(II)···H–N unit **2–5**, as reflected in various data such as $^1J(^{195}Pt,^1H)$ values, can be readily correlated with ligand properties of rigidity and bulk. In **2b** containing the rigid ligand I, the $^1J(^{195}Pt,^1H)$ value is the largest, i.e. 180 Hz, whereas, in **3** containing II with the flexible –CH_2NHMe_2 moiety, this coupling constant is more than halved to 75 Hz. Platinum complex **5** has an intermediate rigidity because of the Me substituent on the benzylic C atom of ligand IV and has an intermediate $^1J(^{195}Pt,^1H)$ value of 104 Hz. As regards steric bulk on the N atom, complex **4** containing ligand III with an –NEt$_2$ unit has a smaller $^1J(^{195}Pt,^1H)$ value than complex **3** containing ligand II with a less bulky –NMe$_2$ unit. The explanation for these results is that even with wagging of the aromatic skeleton,[47] the ammonium moiety of the more rigid ligand skeletons is held more fixedly near the Pt center. With a more flexible system, the H atom on nitrogen can more easily move about above the metal coordination sphere to find a situation that is a balance of steric and electronic factors. Furthermore, the effect of increasing bulk on the ammonium moiety is to push this unit further out of the metal coordination sphere. The result of these variations in ligands I–IV, reflected in the ^{1}H NMR and IR data,[36] is that a strengthening of the Pt···H interaction is attended by a weakening of the N–H bond. Similar effects have also been found to affect the reactivity of analogous iridium complexes.[12] In contrast to **3** and **4**, the complex [Pt_2{$C_6H_3(CH_2NHMe_2)_2$-2,6-*C*}$_2I_4$][CF_3SO_3]$_2$ shows no Pt···H–N interactions of the flexible –CH_2NHMe_2 moieties with the Pt center, and this may be a consequence of the electronegative iodide ligands making the Pt center less electron rich than that in either **3** or **4**.[48]

---

(40) Wilkinson, G.; Stone, F. G. A.; Abel, E. W. *Comprehensive Organometallic Chemistry*; Pergamon Press: New York, 1982; Vol. 2.

(41) For example: (a) Kawakami, K.; Okawara, R. *J. Organomet. Chem.* **1966**, *6*, 249. (b) Elschenbroich, Ch.; Salzer, A. *Organometallchemie*, 2nd ed.; B. G. Teubner: Stuttgart, Federal Republic of Germany, 1988.

(42) (a) Blake, D. M.; Kubota, M. *Inorg. Chem.* **1970**, *9*, 989. (b) Crabtree, R. H.; Quirk, J. M.; Fillebeen-Khan, T.; Morris, G. E. *J. Organomet. Chem.* **1979**, *181*, 203. (c) Imhoff, P.; Nefkens, S. C. A.; Elsevier, C. J.; Goubitz, K.; Stam, C. H. *Organometallics* **1991**, *10*, 1421.

(43) (a) Romeo, R.; Minniti, D.; Lanza, S.; Uguagliati, P.; Belluco, U. *Inorg. Chem.* **1978**, *17*, 2813. (b) Belluco, U.; Michelin, R. A.; Uguagliati, P.; Crociani, B. *J. Organomet. Chem.* **1983**, *250*, 565.

(44) Crociani, B.; Di Bianca, F.; Giovenco, A.; Scrivanti, A. *J. Organomet. Chem.* **1983**, *251*, 393.

(45) (a) Ryabov, A. D. *J. Organomet. Chem.* **1984**, *268*. 91. (b) Ryabov, A. D. *Inorg. Chem.* **1987**, *26*, 1252.

(46) (a) Louw, W. J.; de Waal, D. J. A.; Chapman, J. E. *Chem. Commun.* **1977**, 845. (b) Ashworth, T. V.; Singleton, J. E.; de Waal, D. J. A.; Louw, W. J.; Singleton, E.; van der Stok, E. *J. Chem. Soc., Dalton Trans.* **1978**, 340.

(47) For square-planar d^8 metal complexes containing ortho-substituted aryl groups, there is ample evidence that full rotation by 180° around the C_{ipso}–M bond can be blocked. This is particularly true in systems where a cis-positioned ligand is 'fixed', as here, by chelation. See for example: Terheijden, J.; van Koten, G.; Muller, F.; Grove, D. M.; Vrieze, K.; Nielsen, E.; Stam, C. H. *J. Organomet. Chem.* **1986**, *315*, 401.

(48) Davidson, M. F.; Grove, D. M.; van Koten, G.; Spek, A. L. *J. Chem. Soc., Chem. Commun.* **1989**, 1562.

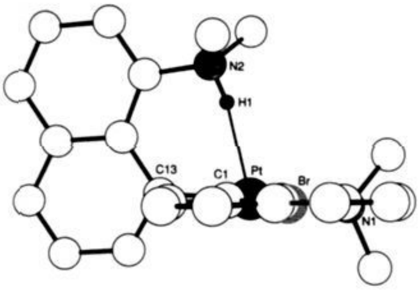

Figure 5. View of **2b** perpendicular to the protonated ligand.

Type of Interaction in the Bridging-Hydrogen Complexes. The three-center interaction shown in this paper, i.e. an N–H bond with a metal center, has been described in literature only a few times before and has been described in different ways. For example, the Pt···H–N unit in *cis*-Pt(*o*-$Ph_2PC_6H_4NC(O)C_6H_4$)(*o*-$Ph_2PC_6H_4NHC(O)Ph$) was described as 'agostic', suggesting a three-center two-electron interaction.[8] However, in [N(*n*-$Pr)_4]_2[PtCl_4]$·[*cis*-$PtCl_2(NH_2Me)_2$], a three-center four-electron interaction including an electrostatic component was proposed as being the nature of the *inter*molecular Pt···H–N bridge.[7] Although extended Hückel molecular orbital calculations do not take care of electrostatic energy, Midollini et al. deduced from this type of calculation on a model system of the d^{10} Ni complex [$(Hnp_3)NiCO][BPh_4$] ($Hnp_3 = NH(CH_2CH_2PPh_2)_3$) (whose X-ray molecular structure contains a Ni···H–N unit and whose ^1H NMR spectrum shows the N–H proton at 14.6 ppm) that electrostatic forces are important in the Ni···H–N interaction.[9] The characteristics of our complex **2b** are all in agreement with the type of interaction described for both [N(*n*-$Pr)_4]_2[PtCl_4]$·[*cis*-$PtCl_2(NH_2Me)_2$] and [$(Hnp_3)NiCO][BPh_4$]. The *intra*molecular Pt···H–N bridge in **2b** (see Figure 5) is close to linear (∠Pt–H–N = 168.0 (4)°), and the acidic proton has an extremely downfield ^1H NMR shift; both observations being typical for a three-center four-electron interaction. Furthermore, the significantly shifted ν(N–H) in the IR spectrum of **2b** (2100 cm^{-1}) is more like that found for [$(Hnp_3)NiCO][BPh_4$] than that found for the agostic system of *cis*-Pt(*o*-$Ph_2PC_6H_4NC(O)C_6H_4$)(*o*-$Ph_2PC_6H_4NHC(O)Ph$) (3150 cm^{-1}).[8] The Pt···H–N moiety in **2–4** can, therefore, best be described as a three-center four-electron interaction either with or without an electrostatic component. Theoretical calculations on the model system [$PdCl(Me)_2$-(NH_3)···H–NH_3] show that orbital interaction between the metal center and the HNH_3 unit (three-center four-electron interaction) is quite minimal though the electrostatic interaction is maximized.[19] The fact that in **6** a type of Br···H–N bridge is formed, which originates from electrostatic attraction (as does an additional Cl···H–C bridge in [N(*n*-$Pr)_4]_2[PtCl_4]$·[*cis*-$PtCl_2(NH_2Me)_2$]),[7] is further evidence for the importance of the electrostatic component of the interaction.

As shown in Figure 5, the bridging proton of **2b** is held by an internal amine function above an almost perfectly planar metal coordination sphere and one can view this complex as a (homogeneous) model system for a metal surface to which a hydrogen is bound, i.e. a heterogeneous catalyst for reactions such as hydrogenation or hydroformylation.

Conclusions

A series of new complexes containing a unique Pt···H–N moiety has been synthesized and characterized. Combined spectroscopic, structural, and theoretical data suggest that the Pt···H–N interaction is mainly due to electrostatic forces. The strength of this interaction is influenced not only by steric hindrance present around the N donor atom but also by ligand rigidity. More steric hindrance causes a larger interaction and a larger $^{195}Pt-^1H$ coupling constant. The latter has an almost reciprocal relation both with the $^{15}N-^1H$ coupling constant *and* with ν(N–H). Although the strength of the interaction is different for each ligand system, the stability of the complexes remains similar. One exception is complex **6** (containing ligand IV), which results from steric interactions of the Me substituent on the benzylic carbon atom with the $-NMe_2$ group. This overcomes the electrostatic preference of the N–H moiety to interact with the Pt center and gives a new interaction of the N–H moiety with the Pt–Br bond. This behavior is extra evidence for the electrostatic component of the interactions of N–H units with metal centers.

This study shows clearly that reactions of d^8 organometallic complexes with HX may afford products other than those expected from oxidative addition. More importantly, every other reaction type concerning protonic hydrogens, e.g. cyclometalation or C–H activation, may involve the intermediacy of species containing M···H–ligand interactions of the type described in this paper. Especially when an amine functionality—or any other group which may act as a reservoir site for protons—is present, the ligand may play a more active role than one may have thought.

Acknowledgment. We gratefully thank Shell Research B.V. (I.C.M.W.-O.) for their financial support. The X-ray data of **2b** were kindly collectecd by A. J. M. Duisenberg. This work was supported in part (A.L.S.) by the Netherlands Foundation for Chemical Research (SON) with financial aid from the Netherlands Organization for Scientific Research (NWO).

Supplementary Material Available: Tables of crystal data, coordinates, isotropic and anisotropic thermal parameters, all H-atom parameters, bond lengths and bond angles for **2b** and **6** (12 pages); listings of observed and calculated structure factors for **2b** and **6** (39 pages). Ordering information is given on any current masthead page.